IXPE
Imaging X-Ray Polarimetry Explorer

The Imaging X-ray Polarimetry Explorer

Martin C. Weisskopf

NASA Marshall Space Flight Center

Presentation to APAC

March 15, 2021

IXPE Deployed

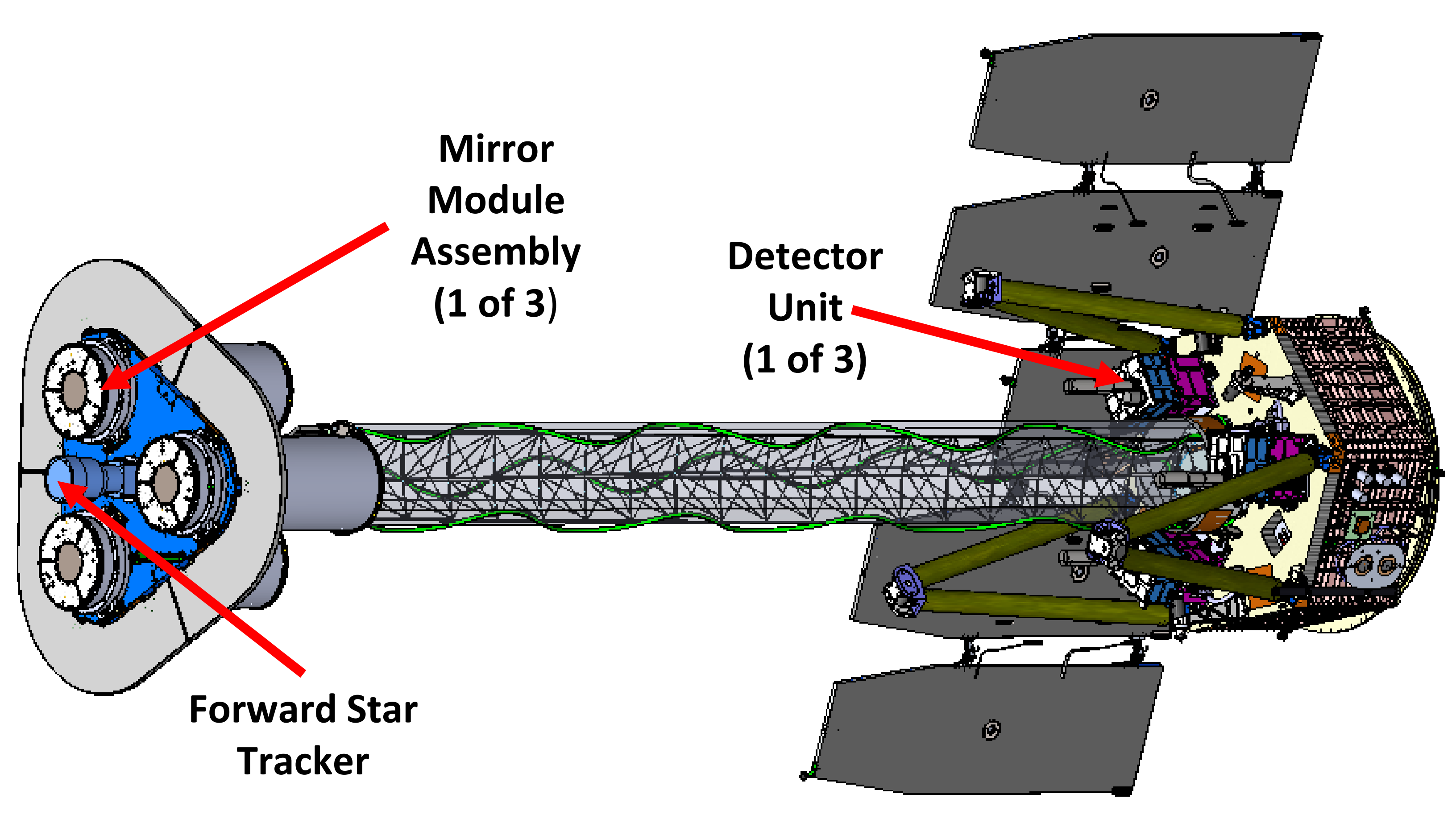

5.2 m total length
4.0 m focal length

IXPE
Imaging
X-Ray
Polarimetry
Explorer

IXPE Exists!

Janice Houston, IXPE Lead Systems Engineer in residence at Ball, with stowed observatory

The IXPE Team

Marshall Space Flight Center: PI team, project management, SE and S&MA oversight, mirror module fabrication, X-ray calibration, science operations, and data analysis and archiving	IAPS, INAF (Istituto Nazionale di Astrofisica / National Institute for Astrophysics), INFN, OAC, OHB Italia: Polarization-sensitive imaging detector systems
	CU, LASP: Mission operations
agenzia spaziale italiana: Detector system funding, ground station	Roma Tre Università degli Studi, Stanford University: Scientific theory
	Nagoya University: Thermal Shields
Ball: Spacecraft, payload structure, payload, observatory I&T	Massachusetts Institute of Technology: Co-Investigator

Science Advisory Team

SAT currently comprises > 90 scientists from 12 countries

IXPE
Imaging X-Ray Polarimetry Explorer

The Science Team

- **Investigators**

  L. Baldini (Co-IPI), W. Baumgartner, R. Bellazzini, S. Bongiorno, E. Costa, J. Kolodziejczak, L. Latronico, H. Marshall, G. Matt, F. Muleri, S. O'Dell, B. Ramsey (DPI), R. Romani, P. Soffitta (IPI), A. Tennant, M. Weisskopf (PI)

- **Collaborators (75 from 12 countries)**

  I. Aguido, L.A. Antonelli, M. Bachetti, S. Bianchi, R. Bonino, A. Brez, N. Bucciantini, F. Capitanio, E. Cavazzuti, E. Churazov, S. Ciprini, M. Cocchi, L. Costamante, A. De Rosa, E. Del Monte, N. Di Lalla, I. Donnarumma, V. Doroshenko, M. Dovčiak, S. Ehlert, T. Enoto, Y. Evangelista, S. Fabiani, J. Garcia, S. Gunji, K. Hayashida, J. Heyl, A. Ingram, W. Iwakiri, S. Jorstad, V. Karas, V. Kaspi, F. Kislat, T. Kitaguchi, H. Krawczynski, M. Kuss, I. Liodakis, G. Madejski, S. Maldera, A. Manfreda, F. Marin, A. Marinucci, A. Marscher, F. Massaro, I. Mitsuishi, T. Mizuno, S. Ng, N. Omodei, C. Oppedisano, L. Pacciani, A. Papitto, G. Pavlov, M. Perri, M. Pesce-Rollins, P.-O. PetruccI, M. Pilia, A. Possenti, J. Poutanen, S. Puccetti,

  M. Razzano, C. Sgrò, P. Slane, G. Spandre, L. Stella, R. Sunyaev, T. Tamagawa, F. Tavecchio, R. Taverna, Y. Tawara, N. Thomas, A. Trois, R. Turolla, J. Vink, K. Wu, S. Zane

The Working Groups

- Science Working Group (SWG)
  - G. Matt (IT) & S. O'Dell (US), Co-Chairs
- Science Advisory Team (SAT)
  - G. Matt (IT) & R. Romani (US), Co-Chairs
- SAT Topical Working Groups (TWG), Leads
  - Pulsar Wind Nebula & Radio Pulsars, N. Bucciantini (IT)
  - Supernova remnants, P. Slane (US)
  - Accreting stellar-mass black holes, M. Dovčiak (CZ)
  - Accreting neutron stars, J. Poutanen (FI)
  - Magnetars, R. Turolla (IT)
  - Radio-quiet AGN and Sgr A*, F. Marin (FR)
  - Blazars & radio galaxies, A. Marscher (US)
- Calibration Working Group
  - W. Baumgartner (US), F. Muleri (IT), & J. Kolodziejczak (US)
- Science Analysis & Simulation Working Group
  - L. Baldini (IT) & H. Marshall (US)

Shield and Collimator Suppress Background

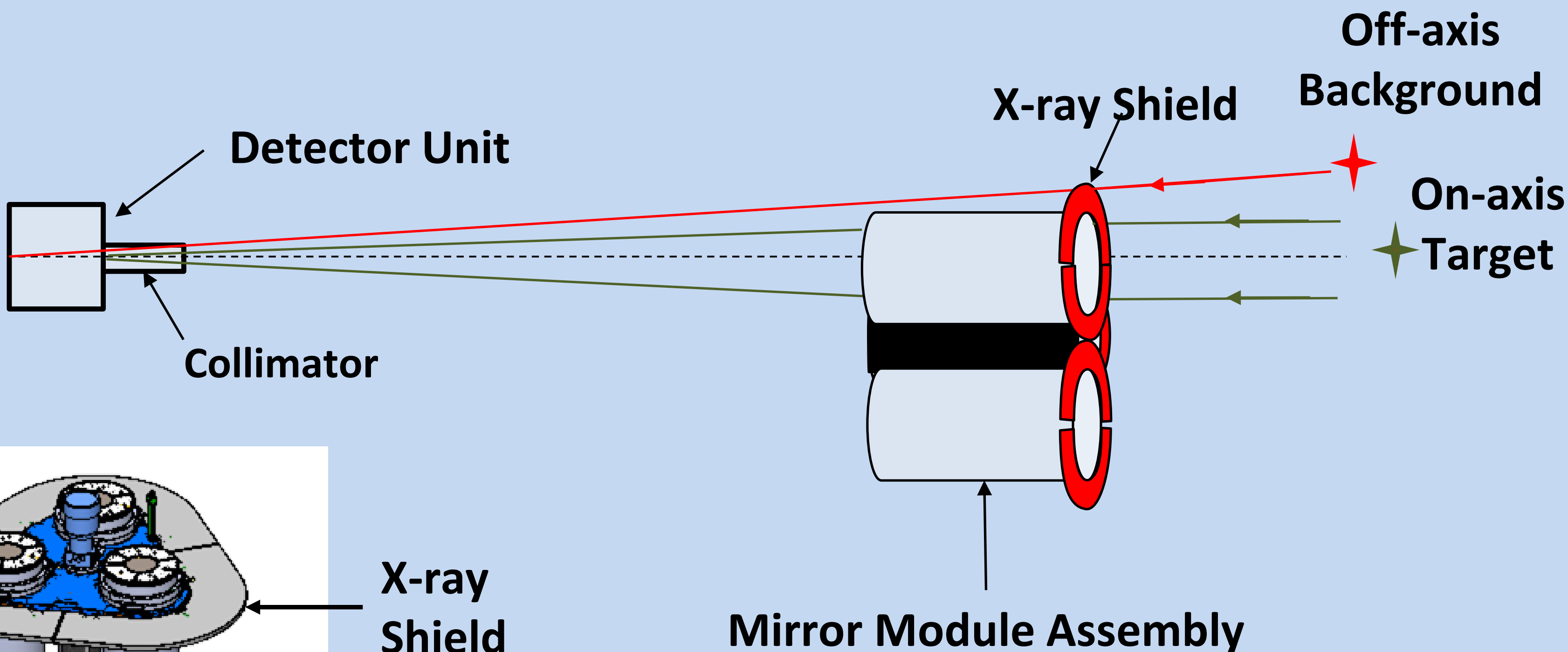

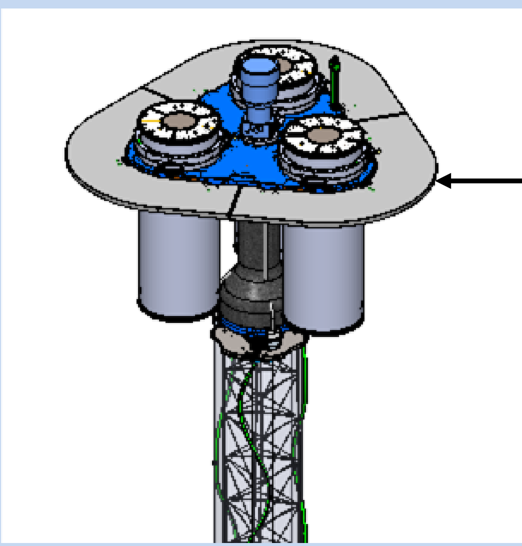

X-ray
Shield

Mirror-Shell Production Process

Mandrel fabrication

1. **Machine mandrel from aluminum bar**

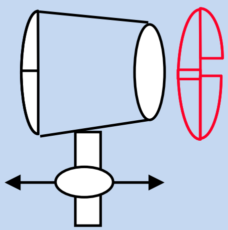

2. **Coat mandrel with electroless nickel (Ni-P)**

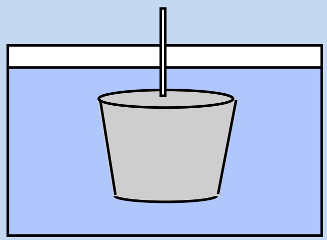

3. **Diamond turn mandrel to sub-micron figure accuracy**

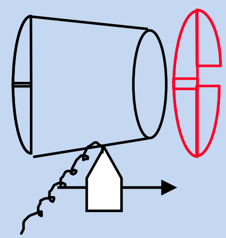

4. **Polish mandrel to 0.3-0.4 nm RMS**

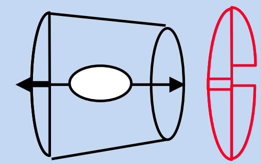

5. **Conduct metrology on the mandrel**

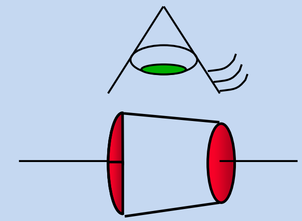

Mirror-shell forming

6. **Passivate mandrel surface to reduce shell adhesion**

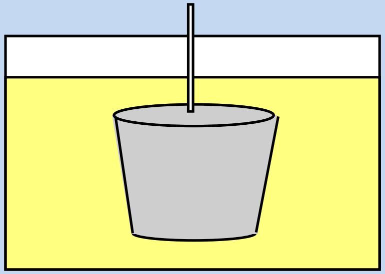

7. **Electroform Nickel/Cobalt shell onto mandrel**

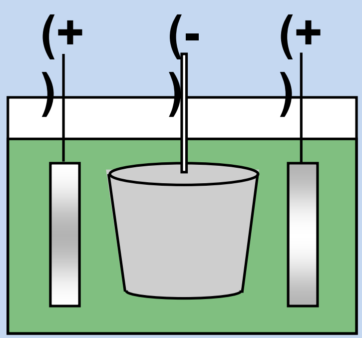

8. **Separate shell from mandrel in chilled water**

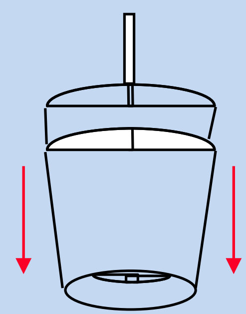

Ni/Co electroformed IXPE mirror shell

IXPE
Imaging
X-Ray
Polarimetry
Explorer

Marshall Space Flight Center

agenzia spaziale italiana

The Optics

Parameter	Value
Number of mirror modules	3
Number of shells per mirror module	24
Focal length	4 m
Total shell length	600 mm
Range of shell diameters	162–272 mm
Range of shell thicknesses	0.16–0.25 mm
Shell material	Electroformed nickel–cobalt alloy
Effective area per mirror module	166 cm^2 (@ 2.3 keV); > 175 cm^2 (3–6 keV)
Angular resolution (HPD)	≤ 27 arcsec
Field of view (detector limited)	12.9 arcmin square

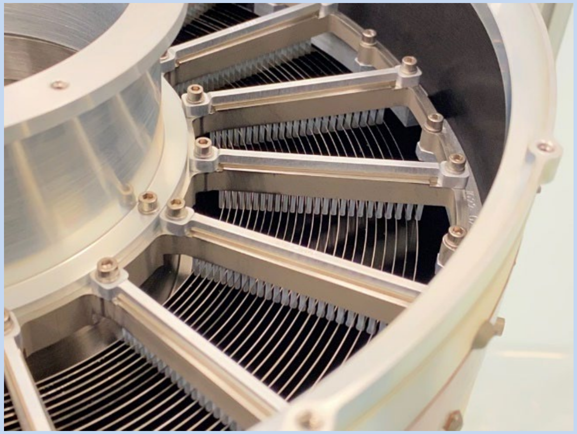
MMA, showing 24 shells

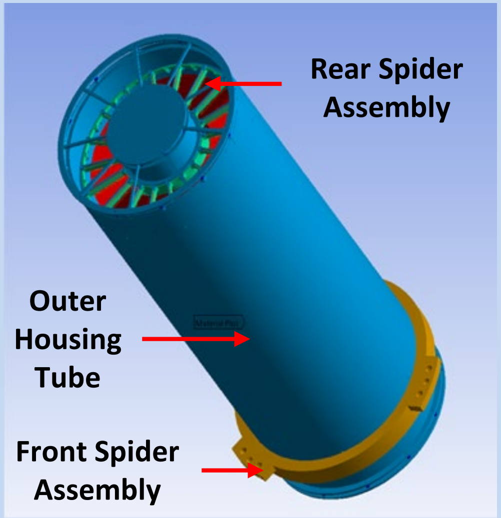


Three IXPE Mirror Module Assemblies


MMA with Thermal Shield on end

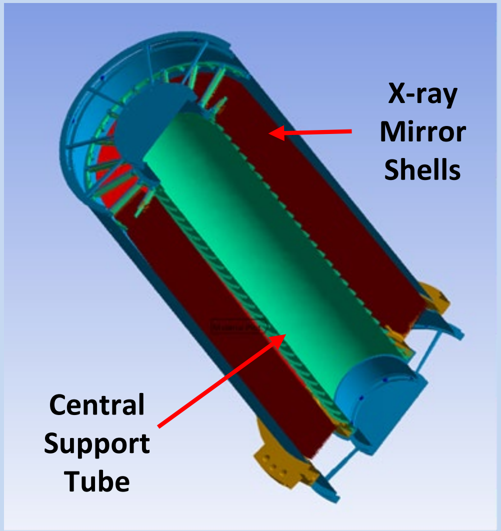

Stray Light Test Facility

- **X-ray calibration of the optics occurred at MSFC's 100-m X-ray test facility**

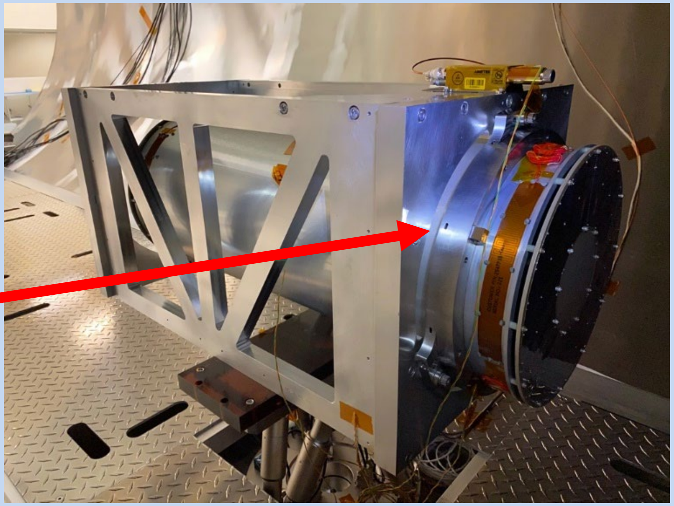

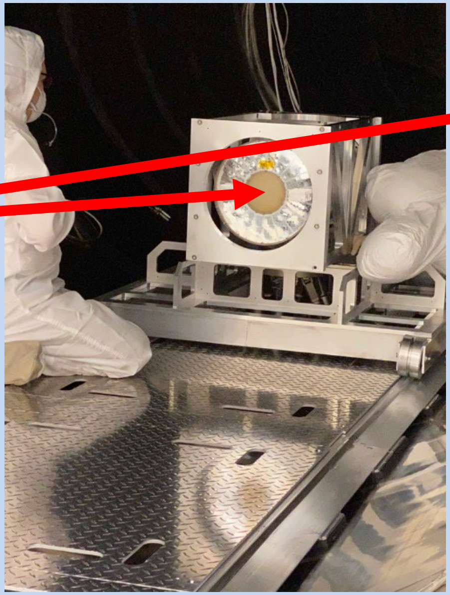

Mirror Module Assembly

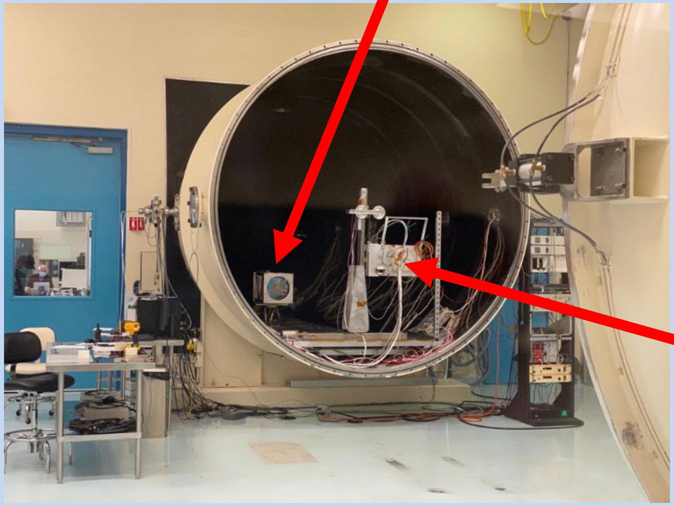

X-Y stage with detector mounting plate

Angular Resolution

MMA	#1	#2	#3
6.4 keV	18.9″	24.8″	24.2″
4.5 keV	18.9″	25.0″	26.9″
2.3 keV	18.7″	24.5″	26.7″

Values in the table are half-power diameters (HPDs) for the individual MMAs alone. After adjustment for alignment errors, detector resolution, focus, etc., the on-orbit system-level resolution is 28″.

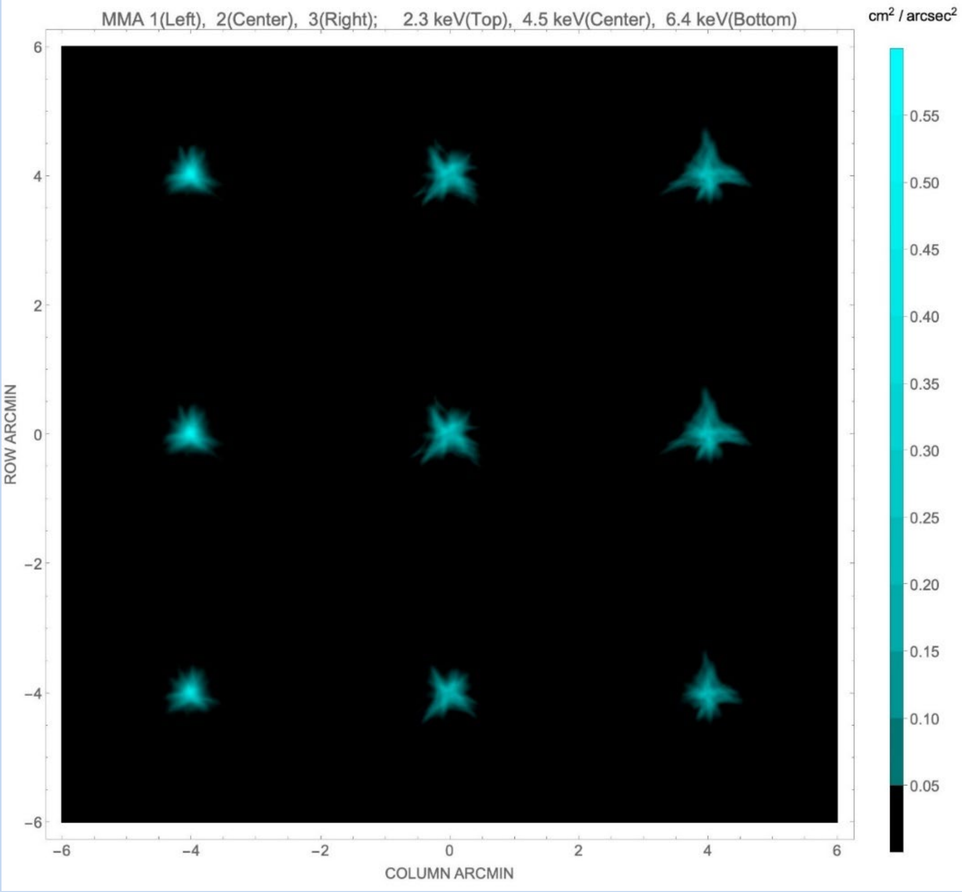

At-focus images for MMA1, MMA2 and MMA3 (left to right) taken at 2.3 keV, 4.5 keV and 6.4 keV (top to bottom).

Imaging polarimetry

- **IXPE 30" half-power diameter on Chandra image of the Crab Nebula**

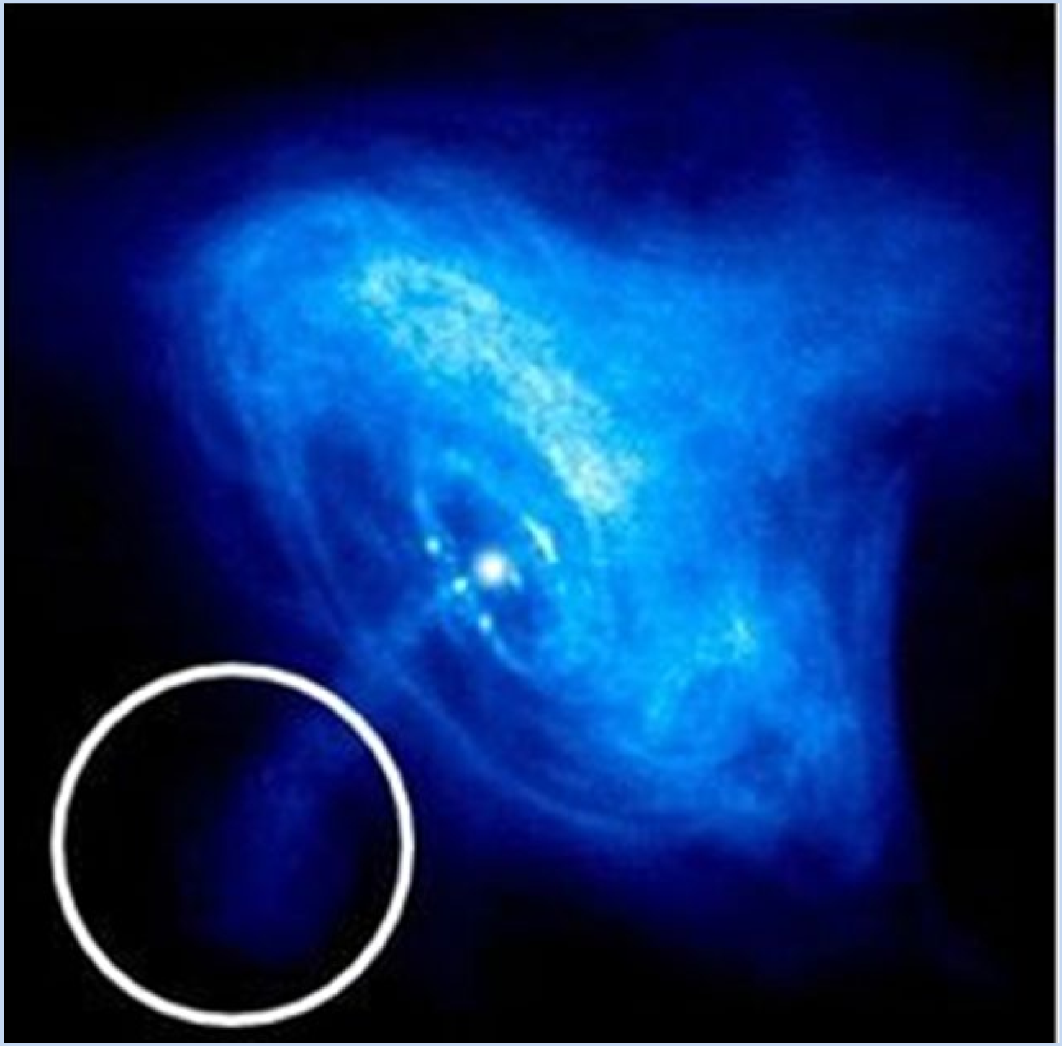

Detection Principle

- **The detection principle is based upon the photoelectric effect**

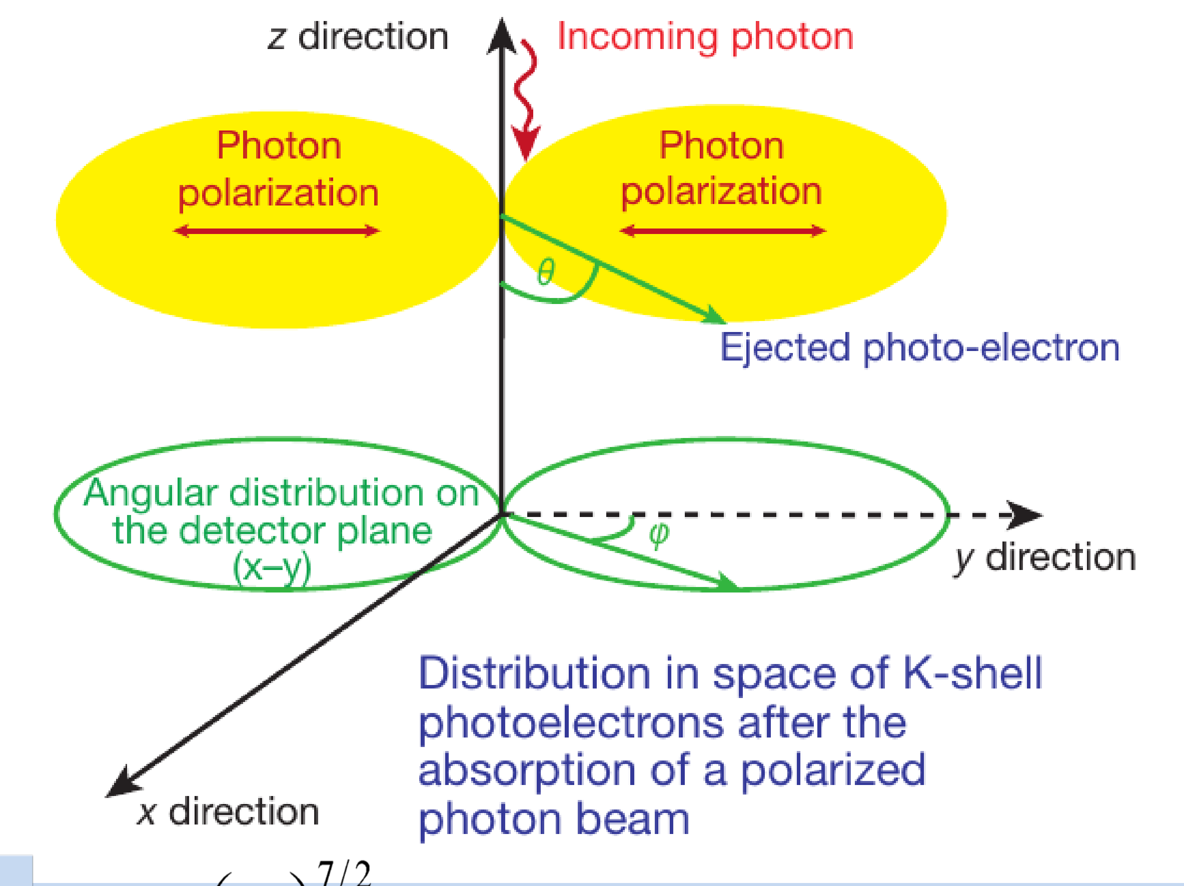

$$\frac{d\sigma}{d\Omega} = r_0^2 Z^5 \alpha_0^4 \left(\frac{1}{\beta}\right)^{7/2} 4\sqrt{2}\sin^2\theta\cos^2\varphi \text{ , where } \beta \equiv \frac{E}{mc^2} = \frac{h\nu}{mc^2}$$

The Detector

- **The initial direction of the K-shell photoelectron is determined by the orientation of the incident photon's electric vector**

X Rays In

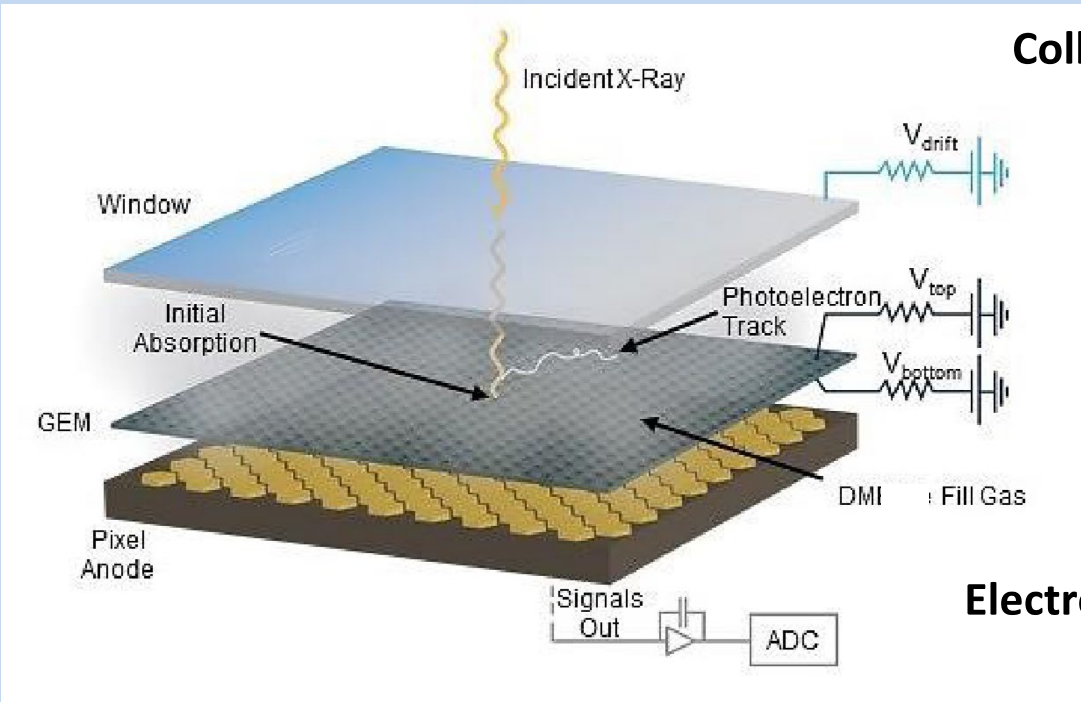

Collimator

Gas Pixel Detector

Electronics

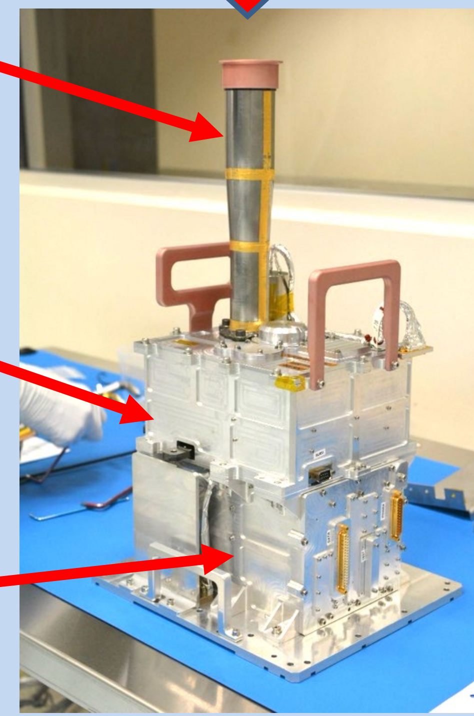

- **The distribution of the photoelectron initial directions measures the degree of polarization and the position angle**

IXPE
Imaging X-Ray Polarimetry Explorer

Detector Properties

Parameter	Value
Sensitive area	15 mm × 15 mm (13 x 13 arcmin)
Fill gas and asymptotic pressure	DME @ 0.656 atmosphere
Detector window	50-µm thick beryllium
Absorption and drift region depth	10 mm
GEM (gas electron multiplier)	copper-plated 50-µm liquid-crystal polymer
GEM hole pitch	50 µm triangular lattice
Number ASIC readout pixels	300 × 352
ASIC pixelated anode	Hexagonal @ 50-µm pitch
Spatial resolution (FWHM)	≤ 123 µm (6.4 arcsec) @ 2 keV
Energy resolution (FWHM)	0.57 keV @ 2 keV ($\propto \sqrt{E}$)
Useful energy range	2 - 8 keV

The Detectors

- The Detectors mounted to the spacecraft top deck at Ball Aerospace

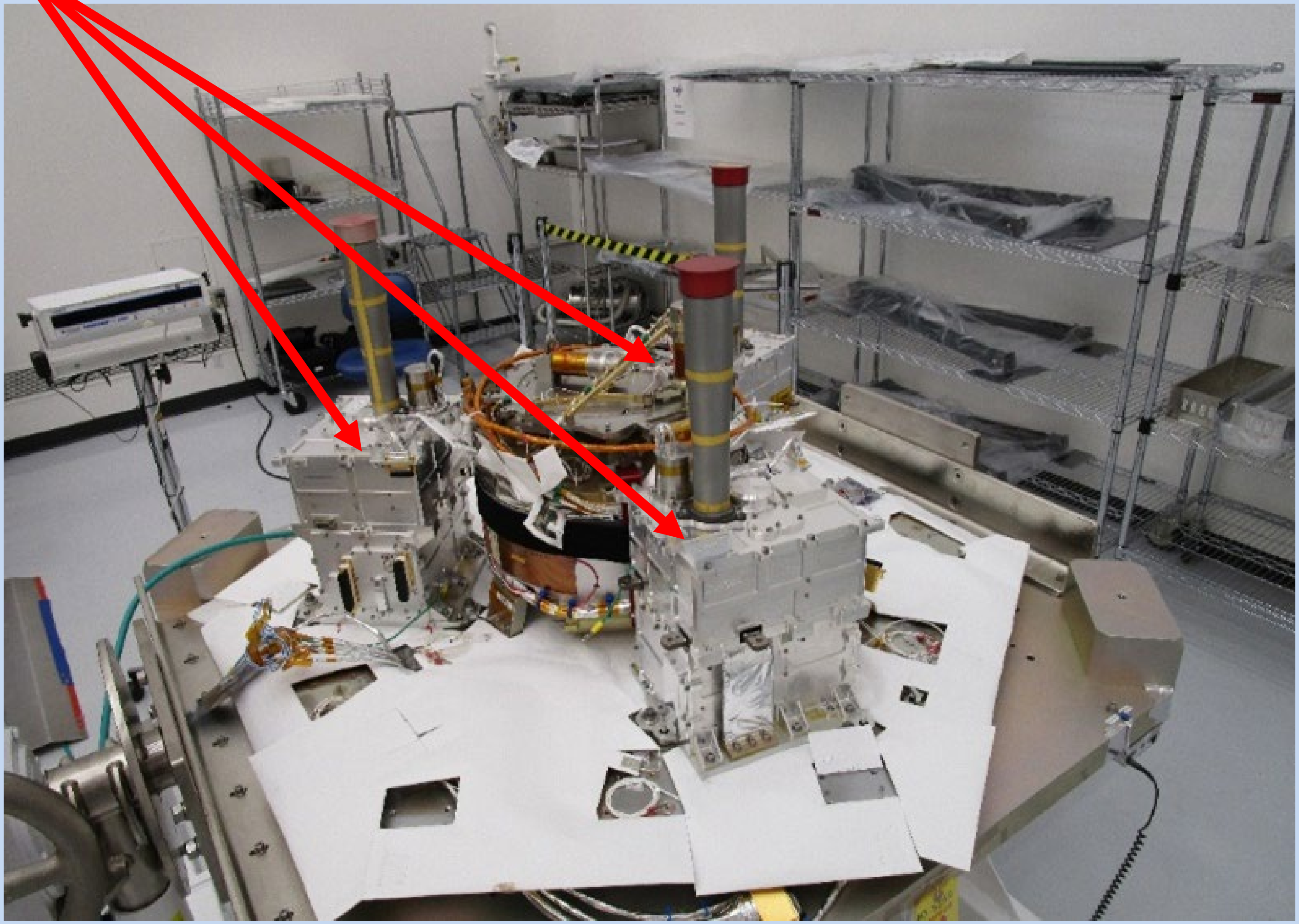

Filter Calibration Wheel Assembly

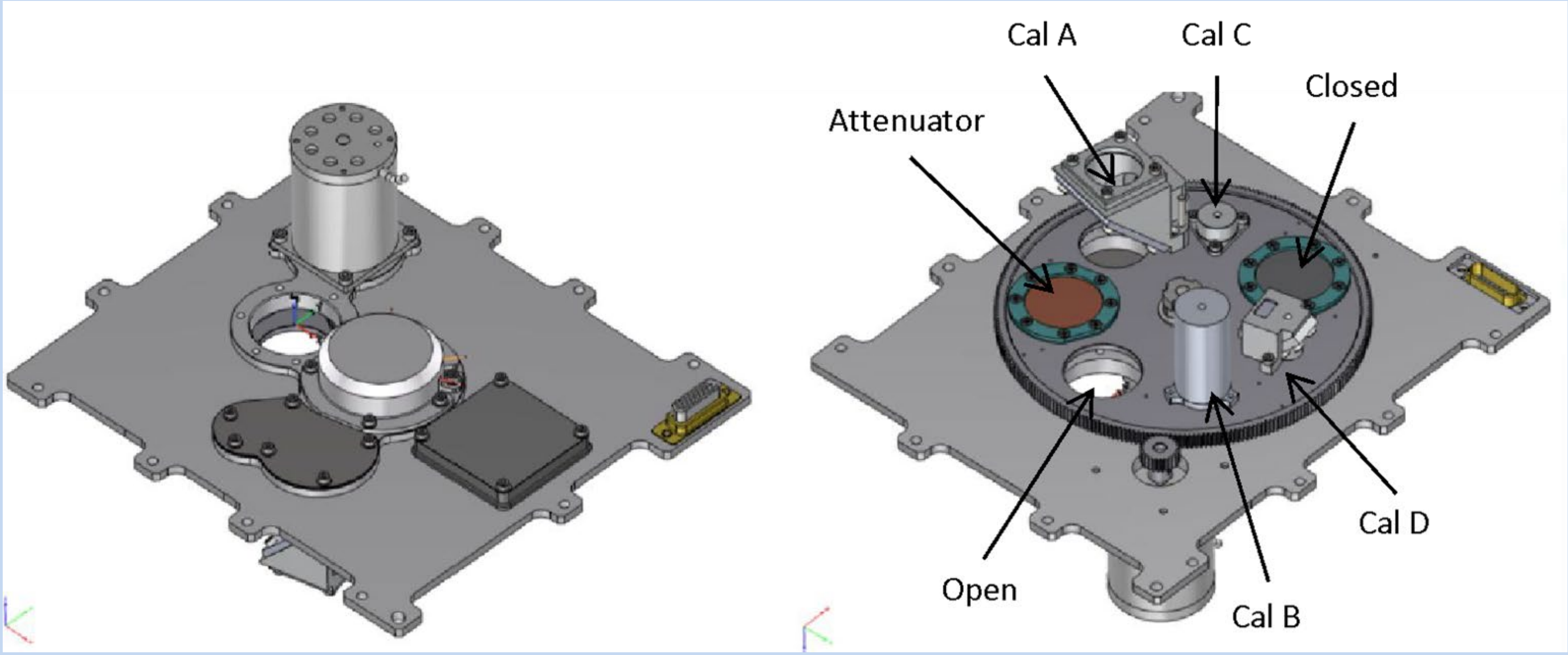

Filter and Calibration Wheel (FCW), providing open, attenuated, and closed positions, plus four ^{55}Fe-powered calibration sources:

- **Cal A – Bragg-reflected polarized 2.98-keV (Ag-Lα fluorescence) and 5.89-keV (Mn-Kα)**
- **Cal B – unpolarized 5.89-keV spot**
- **Cal C – unpolarized 5.89-keV flood**
- **Cal D – unpolarized 1.74-keV (Si-Kα fluorescence) flood**

Minimum Detectable Polarization (MDP)

$$MDP_{99}(\%) = (4.29x10^4 / M(\%))\sqrt{(R_S + R_B)} / \sqrt{R_S^2 t}$$

- R_S is the observed source counting rate
- R_B is the observed background counting rate
- t is the integration time
- M is the modulation factor—i.e., the amplitude of the variation of the ensemble of position angles for a 100%-polarized source

Neural-Network Analysis

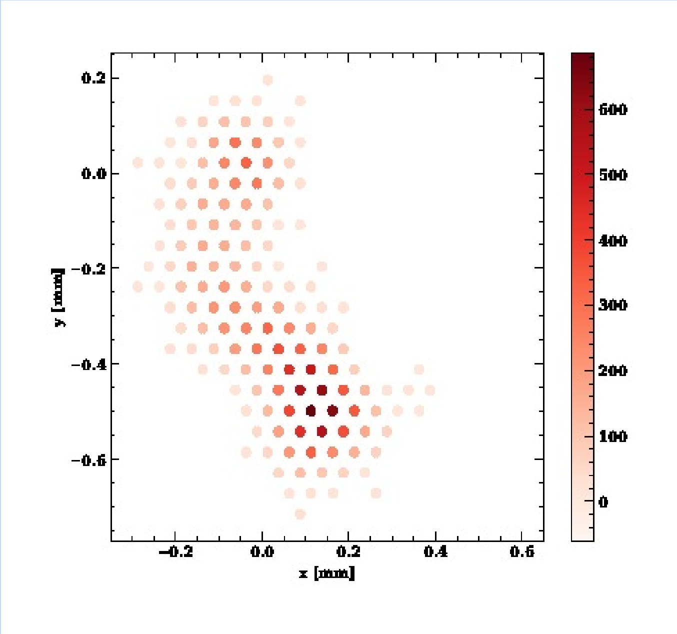

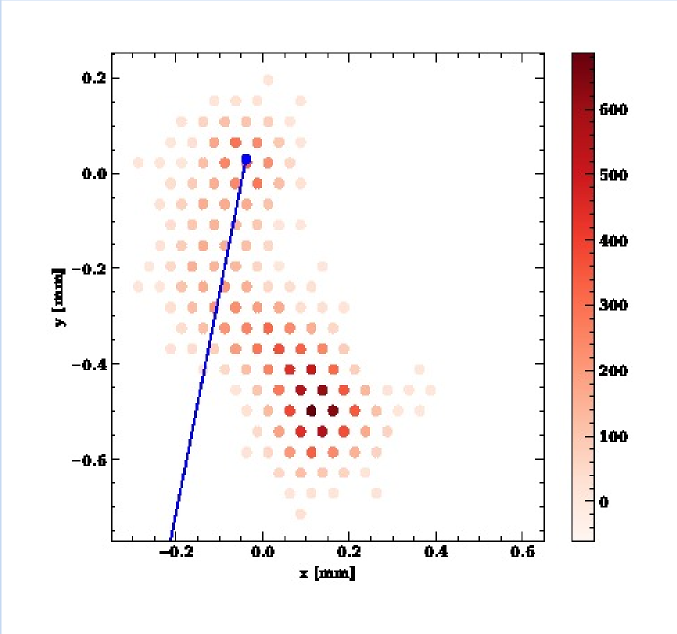

- **Baseline moments analysis is a simple, effective, long-studied and well-understood method of extracting information from ionization tracks made by the photo-electron in the detector gas**
- **Machine Learning (neural-network) techniques can extract more information from each track**
  - **Improves position-angle (PA) measurements, especially at higher energies**
  - **Allows one to compute statistical and reconstruction errors for each event**
  - **Mildly improves estimates of the energy and conversion point of each event**

First Year's Mission — Release 1

- **Next version will be released 6 months prior to launch**
- **Observing plan is from input from the IXPE Science Advisory Team**
  - **Seven Topical Working Groups (TWG), based upon category of source**
- **Needed exposure times assume moments-method event reconstruction**
  - **Will increase somewhat, based upon results from recent calibration**
- **However, neural-network event reconstruction will enhance the sensitivity**
  - **Improves MDP_{99} by ~15% (relative) for fixed exposure time**
  - **Reduces**

Source Category	# Sources	Time (Ms)
Pulsar Wind Nebulae	3	2.6
Supernova Remnants	3	3.0
Accreting Neutron Stars	8	1.8
Accreting Black Holes	2	0.6
Magnetars	2	2.0
Radio Quiet AGN and Sgr A*	4	2.8
Blazars and Radio Galaxies	11	3.2
ToOs	6	3
Total	39	19

Radio Pulsars

- **Radio Pulsars**
  - **Perform X-ray phase-resolved polarimetry to test models for a radio pulsar's X-ray emission**
    - **Crab Pulsar — grey is optical, blue is IXPE**

Emission geometry and processes are still unsettled.

- **Competing models predict differing polarization behavior with pulse phase.**

X-rays provide a clean probe of geometry.

- **Absorption likely more prevalent in visible band.**
- **Radiation process entirely different in radio band.**
  - **Recently discovered _no_ pulse phase-dependent variation in polarization degree and position angle @ 1.4 GHz.**
- **140-ks observation of the Crab pulsar gives ample statistics to track polarization degree and position angle.**

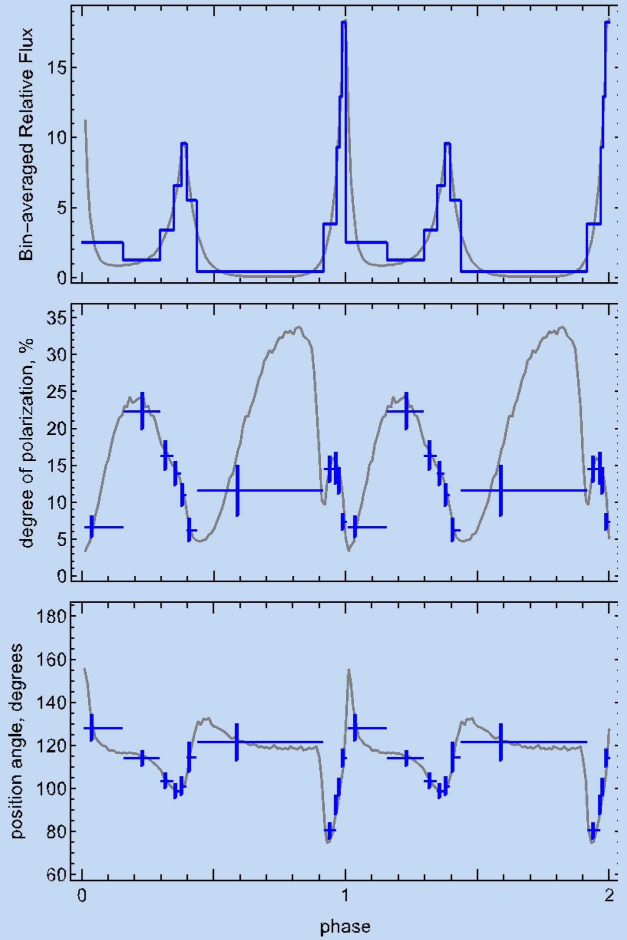

Microquasars

- **Microquasars**
  - **Perform X-ray spectral polarimetry on microquasars to use the position angle to help localize the emission site (accretion disk, corona, jet) and determine the spin**

For a microquasar in an accretion-dominated state, scattering polarizes the disk emission.

Polarization rotation versus energy is greatest for emission from inner disk.

– Inner disk is hotter, producing higher energy X-rays.

Disk orientation from other experiments may be used to constrain GRX1915+105 model.

a = 0.50±0.04; 0.900±0.008; 0.99800±0.00003 (200-ks observation)

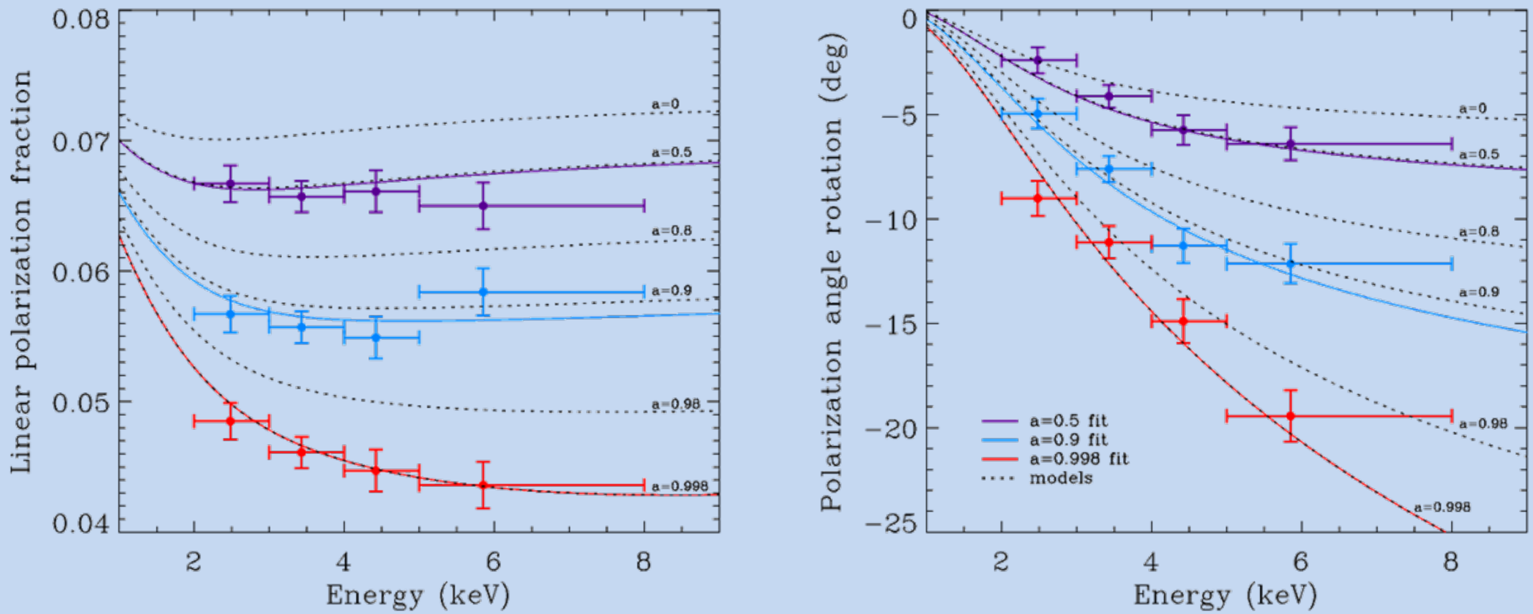

Active Galaxies: Cen A

- **Active galaxies powered by supermassive black holes with jets**
  - **Radio polarization implies the magnetic field is aligned with jet**
  - **Different electron-acceleration models predict different dependences in X-rays**

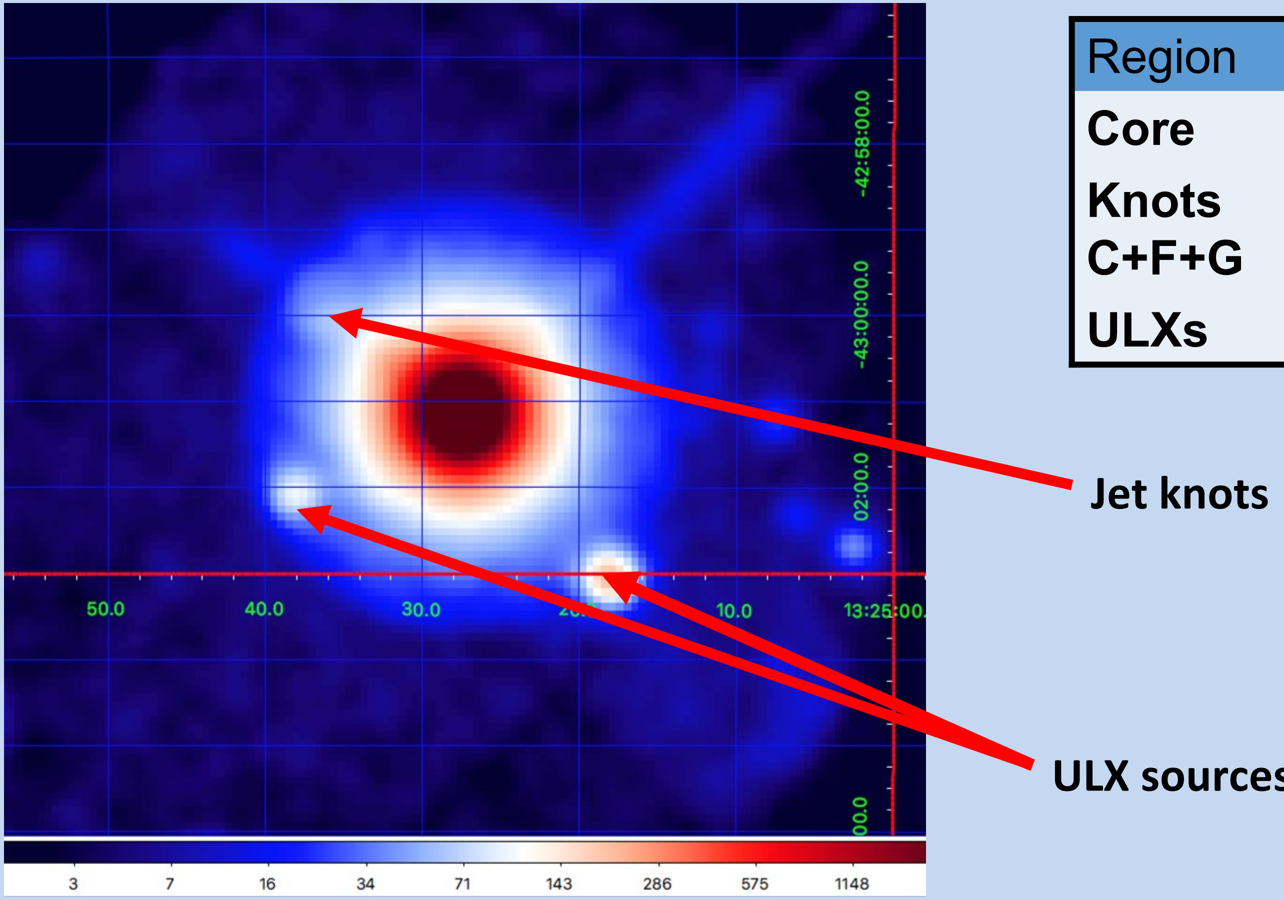

Region	MDP_{99}
Core	**1.4%**
Knots C+F+G	**21%**
ULXs	**25%, 15%**

IXPE
Imaging X-Ray Polarimetry Explorer

Test QED

- **Study magnetars (pulsing neutron stars with magnetic fields up to 10^{15} Gauss)**
  - **Non-linear QED predicts magnetized-vacuum birefringence**
    - **Refractive indices of the two polarization modes differ from 1 and from each other**
    - **Impacts polarization and position angle as functions of pulse phase, but not the flux**
    - **Example is 1RXS J170849.0-400910, with an 11-s pulse period**
    - **Can exclude QED-off at better than 99.9% confidence in 250-ks observation**

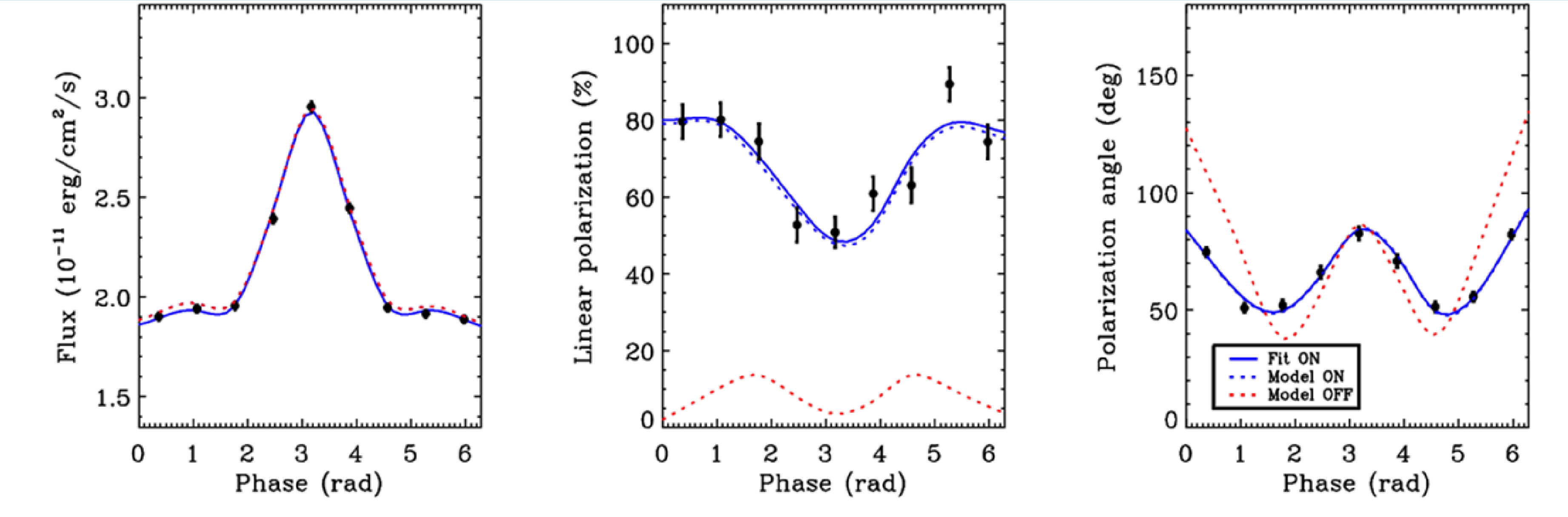

Conclusion

We are keenly looking forward to opening this new window on the sky by adding image resolved polarimetry to the arsenal of tools to study the X-ray emission from astrophysical sources.

Scheduled launch date is 2021 November 17!